






Smoke detection in images through fractal dimension-based binary classification

Javier Del-Pozo-Velázquez^a, Javier Manuel Aguiar-Pérez^{a,*} , Pedro Chamorro-Posada^{a,b} ,
María Ángeles Pérez-Juárez^a , Xinheng Wang^{c,d} , Pablo Casaseca-de-la-Higuera^{a,e} 

^a Departamento de Teoría de la Señal y Comunicaciones e Ingeniería Telemática, Universidad de Valladolid, ETSI Telecomunicación, Paseo de Belén 15, 47011 Valladolid, Spain

^b Laboratory for Disruptive Interdisciplinary Science (LaDIS), Universidad de Valladolid, Spain

^c CIP Technologies Ltd, United Kingdom

^d Xi'an Jiaotong-Liverpool University (XJTLU), United Kingdom

^e Laboratorio de Procesado de Imagen, Universidad de Valladolid, ETSI Telecomunicación, Paseo Belén 15, 47011 Valladolid, Spain

ARTICLE INFO

Keywords:

Early fire detection
Fractal dimension
Image classification
Remote Sensing

ABSTRACT

Early fire detection is crucial for enabling rapid response and minimizing potentially catastrophic consequences. While artificial intelligence-based approaches have been developed for this task, they often demand substantial computational resources. Moreover, detecting smoke is inherently challenging due to its irregular, heterogeneous texture—especially under adverse weather conditions such as fog or cloud shadows. This paper introduces and validates an efficient smoke detection method grounded in fractal dimension analysis. The proposed approach involves dividing images into tiles, computing the fractal dimension for each block, and analysing the resulting fractal dimension distribution patterns to identify smoke presence. To evaluate its performance, we employed publicly available surveillance images from the High Performance Wireless Research and Education Network (HPWREN). Experimental results across five different scenarios demonstrate that the method achieves an accuracy of 96.87 %, successfully distinguishing between smoke and smoke-free regions—even under visually challenging conditions. By relying on an efficient fractal dimension algorithm, the proposed method is computationally efficient, and manages to capture the intrinsic texture characteristics of smoke, remaining unaffected by environmental noise such as fog and cloud cover.

1. Introduction

Early fire detection is crucial for minimizing damage and safeguarding the environment, industrial infrastructure, human settlements, and lives. However, detecting fires at an early stage can be particularly challenging, as they often ignite in remote or obscured locations beyond direct human observation. Since fires typically generate smoke and flames, detecting smoke in aerial imagery constitutes a promising strategy for early intervention. These images can be acquired through remote sensing technologies, including IoT edge devices equipped with high-resolution cameras, as well as Unmanned Aerial Vehicles (UAV) and satellites. The effectiveness of this approach heavily depends on image quality—high-resolution imagery is essential to extract accurate, actionable insights for timely response.

This paper proposes and validates an efficient method for detecting fire-prone areas by accurately distinguishing between smoke and non-smoke regions. The proposed approach is based on image tiling and the calculation of fractal dimensions across the resulting patches. Specifically, we employ the computational technique proposed by the authors in [1], which enables the direct estimation of fractal dimensions from digital image files. By computing the fractal dimensions of each image block, a clear threshold allowing reliable separation of smoke-affected areas from smoke-free zones is obtained. The method was validated using publicly available imagery from the High Performance Wireless Research and Education Network (HPWREN) [2]. The proposed technique stands out for its simplicity and low computational cost when compared to resource-intensive Artificial Intelligence (AI)-based methods. Additionally, it does not rely on specialized input

* Corresponding author.

E-mail addresses: jpozvel@ribera.tel.uva.es (J. Del-Pozo-Velázquez), javier.aguiar@uva.es (J.M. Aguiar-Pérez), pedro.chamorro@uva.es (P. Chamorro-Posada), mperez@uva.es (M.Á. Pérez-Juárez), H.Wang@ciptechnology.co.uk, xinheng.wang@xjtlu.edu.cn (X. Wang), casaseca@lpi.tel.uva.es (P. Casaseca-de-la-Higuera).

<https://doi.org/10.1016/j.dsp.2025.105346>

Available online 19 May 2025

1051-2004/© 2025 The Authors. Published by Elsevier Inc. This is an open access article under the CC BY-NC-ND license (<http://creativecommons.org/licenses/by-nc-nd/4.0/>).

data, such as geoinformation metadata, making it highly adaptable to a variety of image sources.

Considering the above, the main contributions of the paper are as follows:

- Proposes an effective method for early fire detection by discriminating between smoke and non-smoke areas in surveillance images.
- Successfully uses image tiling and fractal dimension calculation to analyse and detect smoke texture patterns.
- Applies a computational method to estimate the fractal dimension directly from digital image files, based on previous work [1].
- Validates the proposed method through an experimental study using freely available HPWREN imagery, including colour and near-infrared data from mountaintop cameras.
- Demonstrates that the proposed approach is simple, computationally efficient, and suitable for use with high-resolution imagery captured by Internet of Things (IoT) edge devices, UAVs, and satellites.
- Provides an alternative to AI-based methods by eliminating the need for geoinformation metadata and complex model training.

The remaining of the paper is as follows: Section 2 describes recent related work. Section 3 describes the proposed method including 1) image acquisition and preprocessing; 2) image tiling; 3) fractal dimension calculation of the resulting image blocks; and 4) analysis of the evolution of the fractal dimension for smoke detection. Section 4 presents the experimental results obtained in different smoke detection case studies developed using images from the HPWREN website [2]. Finally, the main conclusions are presented in Section 5.

2. Related work

Detecting smoke in images presents a set of persistent challenges, primarily due to the amorphous and dynamic nature of smoke itself. Unlike well-defined objects, smoke lacks consistent shape or contour, often mimicking the textures and visual patterns of elements such as water, clouds, open skies, or forestry. This visual ambiguity undermines the effectiveness of conventional techniques like background subtraction or basic pattern matching, which rely heavily on structural regularities. As a result, researchers have turned to more flexible and robust methods to improve detection accuracy—especially in cases where smoke appears in small or partially obscured regions. On top of that, processing images for this kind of task can be computationally heavy, adding to the overall complexity and making real-time detection even more challenging.

A wide range of Deep Learning (DL) methods have been applied to the detection of fire and smoke in images, with Convolutional Neural Networks (CNNs) emerging as a particularly effective tool in this domain [3]. These networks, inspired by the visual processing of the human eye, consist of multiple layers that automatically extract meaningful features from raw pixels. Convolutional layers are especially well-suited for object detection and are central to models like You Only Look Once (YOLO). For example, [4] employed a pretrained YOLOv5s model to improve smoke detection accuracy even with limited training data. Lightweight CNNs such as MobileNetV3 [5] have also gained popularity for their efficiency, making them suitable for real-time applications. Beyond object detection, some approaches rely on U-Net-based architectures for pixel-level classification in semantic segmentation tasks [6]. More recent models, such as YOLOv8, combine object detection and segmentation capabilities, and have been used both independently and in conjunction with techniques like Slicing-Aided Hyper Inference (SAHI) to enhance performance on high-resolution images [7–9]. Other efforts have leveraged Object-Based Detection Systems (OBDS) built on YOLOv5 for structured detection [10]. Additionally, semantic segmentation networks like DeepLabv3+ have been adopted for precise delineation of smoke regions, further underscoring the expanding role of Artificial Intelligence (AI)-driven techniques in this field [11].

Nonetheless, a key limitation of these models is their reliance on supervised learning, which requires explicit labelling of smoke regions in the training data—often involving labour-intensive manual annotation.

Table 1 presents a comparative overview of previous studies on fire and smoke detection in imagery alongside the proposed approach. The comparison considers key aspects such as the detection method, dataset used, dataset size, preprocessing techniques, and the main advantages and limitations of each method. Across the reviewed works, several recurring limitations exist. Many are sensitive to adverse environmental conditions, which can significantly affect detection performance [4,6–9,11]. Several approaches also involve high technological complexity, making their implementation and deployment more demanding [4–11]. The reliance on large, manually labelled datasets is another common issue [4–11]. Some methods report low precision or depend on multi-modal data, further complicating the detection pipeline [5]. Others show a strong reliance on data augmentation to reach acceptable performance levels [10], and in certain cases, detection accuracy is highly sensitive to image quality [4]. In contrast, the proposed method addresses several of these challenges by offering key advantages: it remains robust under challenging conditions, achieves high precision, and is computationally lightweight. Moreover, it performs effectively without requiring a large training dataset, making it well-suited for real-world scenarios where data and computational resources are limited.

Additionally, the application of AI techniques for object detection in images can pose several challenges, depending on the domain and the nature of the images or objects involved [12]. In fact, applying AI-based methods to the same task addressed by the proposed approach would typically require not only the image data but also supplementary metadata stored in accompanying files. A common example is the use of shapefiles—vector formats that encode the geographic location of objects along with their associated attributes. Preparing a dataset suitable for training and evaluating an Artificial Neural Network (ANN) therefore involves careful consideration of these requirements. Moreover, some objects are inherently difficult to detect using AI due to their variability and heterogeneity, which further complicates the detection process [13].

On the other hand, it is worth highlighting that smoke regions can also be extracted from images using fractal-based approaches, given that smoke exhibits self-similar properties—much like natural phenomena such as water. In a fractal structure, both the whole and its parts share the same statistical characteristics, often emerging from the repetition of simple processes across scales to produce complex, seemingly infinite patterns. Fractals are, by definition, intricate structures that retain their form across different levels of magnification, and this self-similarity has long attracted the attention of scientists and researchers [14–16]. One of the reasons for this widespread interest is the versatility of fractals, which have been applied in a broad range of applications [17–23]. In image processing, for instance, fractal image compression leverages the repetition of patterns within an image to reduce data size. This block-based technique identifies and encodes similarities across regions, demonstrating the practical value of fractal geometry. Similarly, by recognizing smoke as a self-similar fractal phenomenon, detection methods—such as the one proposed in this paper—can be developed to exploit these structural patterns for more effective image analysis.

3. Method for smoke detection using fractal dimension calculation

This section outlines the proposed method, which is divided into four main phases: (1) image acquisition and preprocessing, (2) image tiling, (3) fractal dimension calculation, and (4) analysis of the fractal dimension evolution. First, the region of interest in the original image is extracted and converted to greyscale, as the three-dimensional property of colour information makes the processing heavier [24]. Secondly, the image is divided into smaller tiles to enable localised analysis. Thirdly, the fractal dimension of each tile is calculated to obtain meaningful

Table 1

Comparison of previous studies on fire and smoke detection in images using a range of DL-based methods with the present study.

Year	Article	Method	Dataset	Dataset Length	Preprocessing	Advantages	Disadvantages	Reference
2023	Efficient Detection of Forest Fire Smoke in UAV Aerial Imagery Based on an Improved Yolov5 Model and Transfer Learning	Transfer Learning (YOLOv5s)	UAV-based imagery	2554 images	K-means++ and Resize	Real-Time Detection High Precision	Affected by Adverse Environmental Conditions Affected by Image Quality Technological Complexity	[4]
2023	The Wildfire Dataset: Enhancing Deep Learning-Based Forest Fire Detection with a Diverse Evolving Open-Source Dataset Focused on Data Representativeness and a Novel Multi-Task Learning Approach	Convolutional Neural Network (MobileNetV3)	Wildfire imagery	2700 images	Data Curation and Deduplication	Contemplates Adverse Conditions Innovative Approach	Low Precision Multimodal Data Needs Technological Complexity	[5]
2023	Burned Area Semantic Segmentation: A Novel Dataset and Evaluation using Convolutional Networks	Deep Learning (U-Net Base)	UAV-based imagery	22,500 images	Image Segmentation	Near Real-Time Detection High Precision	Affected by Adverse Environmental Conditions Need for Large Amounts of Data Technological Complexity	[6]
2024	Scrapping The Web for Early Wildfire Detection	Deep Learning (YOLOv8)	Wildfire imagery	10,000 images	Filtering Strategy	Cost-Effective Dataset Near Real-Time Detection	Affected by Adverse Environmental Conditions Manual labelling and Variability Technological Complexity	[7]
2025	YOLO-SIFD: YOLO with Sliced Inference and Fractal Dimension Analysis for Improved Fire and Smoke Detection	Deep Learning (YOLOv8) + SAHI	Fire dataset	11,515 images	Fractal Dimension Analysis to Study the Spatial Arrangement of Fire and Smoke	Near Real-Time Detection High Precision	Affected by Adverse Environmental Conditions Need for Large Amounts of Data Technological Complexity	[9]
2023	Omni-Dimensional Dynamic Convolution Meets Bottleneck Transformer: A Novel Improved High Accuracy Forest Fire Smoke Detection Model	Deep Learning (OBDS based on YOLOv5)	Wildfire imagery	30,420 images	Seasonal Style Transformation and Improved Mosaic Data Augmentation	Contemplates Adverse Conditions Computational Efficiency	Dependence on Data Augmentation Technological Complexity	[10]
2024	A Lightweight Fire Detection Algorithm based on Improved YOLOv8	Deep Learning (YOLOv8)	Fire dataset	8751 images	Data Augmentation Techniques	Near Real-Time Detection High Precision	Affected by Adverse Environmental Conditions Need for Large Amounts of Data Technological Complexity	[8]
2024	Wildfire and Smoke Early Detection for Drone Applications: A Lightweight Deep Learning Approach	Semantic Segmentation (Deeplabv3+)	Fire dataset	9098 images	Data Augmentation Techniques	Near Real-Time Detection High Precision Lightweight Design	Affected by Adverse Environmental Conditions Need for Large Amounts of Data Technological Complexity	[11]
2025	Present Study	Fractal Dimension	Wildfire imagery	316 images	RGB to Greyscale and Image Tiling	Contemplates Adverse Conditions Low Complexity Small Dataset High Precision	Reference Image Needed Only Static Surveillance Validation performed for Still Images	

information for smoke identification. Finally, the evolution of the fractal dimension is analysed to classify each tile as either smoke or smoke-free.

3.1. Image acquisition and preprocessing

There are three essential factors in the selection of the information source: 1) position of the camera, 2) temporal granularity of data acquisition and, 3) quality of the images. Firstly, the camera position

must be static, covering a fire-prone area, usually on high ground, and the lens must remain stationary, without zooming in or out. Also, the higher the quality of the image, the more accurate the fractal dimension calculation will be.

Although several repositories offer wildfire imagery, the above factors must be considered. For this reason, the source images used in this study were obtained from the High Performance Wireless Research and Education Network (HPWREN) [2]. HPWREN is a research initiative that operates a network of over 140 cameras (including colour and near-infrared) and environmental sensors installed on mountaintops across San Diego and South Carolina counties in the United States. The network provides publicly accessible data in near-real time, offering a valuable resource for wildfire monitoring and response. The images analysed in this study were captured at one-minute intervals, ensuring adequate temporal granularity for the proposed method. The only worth noting limitation of the dataset is the relatively low image resolution (96 dpi), which could potentially impact the precision of the fractal dimension calculations. However, this limitation did not significantly affect the results obtained.

Once the data source had been selected, the images were pre-processed to ensure accurate fractal dimension calculation. Initially, the raw images included elements—such as the sky and camera edges—that could introduce outliers into the analysis. However, because the camera position remains fixed, a cropping step using predefined coordinates was applied to consistently remove these irrelevant regions. Next, the cropped images were converted to greyscale, following findings in [1] that support improved accuracy in fractal dimension calculation when using greyscale images (instead of coloured) during the involved sub-sampling process.

3.2. Image tiling

To enable fractal dimension calculation [25], images were divided into equally sized tiles. Methods such as Quadtree-based tiling or filter-based techniques like the Boxcar method used in [26] were not suitable, as they alter the structural consistency of the image blocks. Instead, a straightforward uniform splitting technique was employed, dividing each image into a 6×6 grid, resulting in 36 tiles with consistent size and resolution for analysis.

3.3. Fractal dimension calculation

After completing the steps detailed in Sections 3.1 and 3.2, the fractal

dimension of the resulting tiles is estimated using the previously proposed compression fractal dimension algorithm [1].

The amount of information S required to represent a fractal object follows the asymptotic scaling

$$S(s) \sim 2^{H(s)} \sim s^D, \quad (1)$$

where s is the scale level, H is the Shannon entropy, and D is the fractal dimension. The definition of the compression dimension follows as

$$D_c = \lim_{s \rightarrow \infty} \frac{\log S(s)}{\log s}. \quad (2)$$

To estimate D_c , a series of representations of the image at different scales is produced by resizing the initial tile by a percentage ranging from 10 % to 90 % with a 10 % increment. This operation is performed using the free ImageMagick library [27]. At each scale, S is estimated from the compressed file size obtained using GZIP (GNU Zip). The fractal dimension is then evaluated from the slope of the linear regression fit of the logarithm of the resizing scale against the logarithm of the compressed sizes.

Whereas in an ideal fractal self-similarity is found at all scales, in any real fractal this range of scales is limited. In our case, such a physical limit is imposed by the limited resolution of the image, as illustrated in Fig. 1. The compression dimension algorithm will only provide a good estimate of the fractal dimension if the image file constitutes a reliable representation of the fractal object at all the scales analysed [1]. Although the rescaling ideally ranges from 10 % to 90 %, an exhaustive study shows that for the tiles used, there is a turning point where the linearity disappears indicating the violation of Eq. (2). For this reason, in this research work, the scaling varies between 50 % and 90 %, i.e., the reduced information content in the scaled versions with resizing percentages between 40 % and 10 % yields meaningless data.

Fig. 1 shows the described slope deviation for a sample image from the first scenario presented in Section 4. A noticeable deviation in the slope of the $\log_2(S)$ vs. $\log_2(s)$ plot, used to compute the fractal dimension, can be observed at the smallest values of s . This deviation is due to the limited resolution of the image and restricts the range of scales s that can be used to estimate the fractal dimension.

3.4. Analysis of the evolution of the fractal dimension

After computing the fractal dimension for each tile, an evolution analysis is carried out to detect smoke within sequences of images from the same scenario. The presence of smoke tends to blur textures and

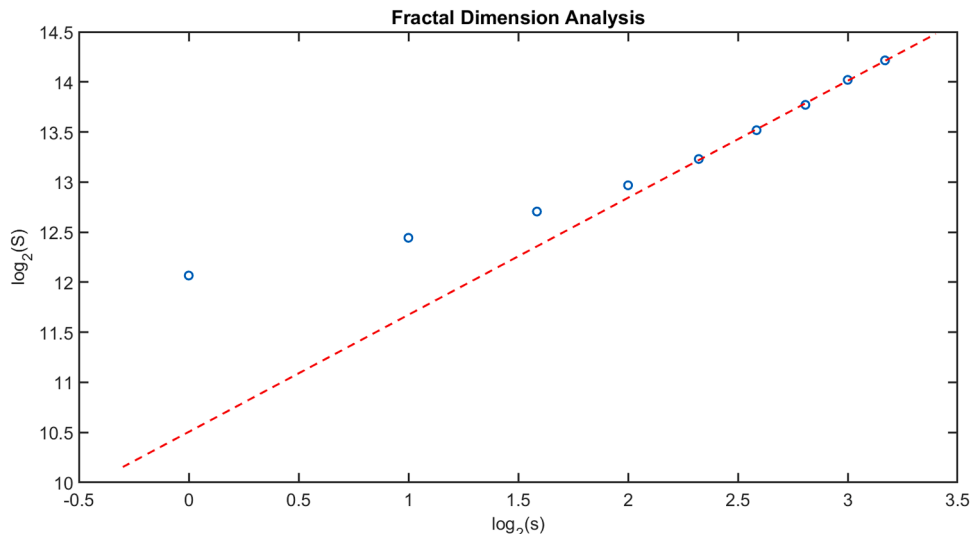


Fig. 1. Fractal dimension analysis along scaled versions.

alters the fractal dimension of affected tiles. As smoke spreads through the scene, these changes become increasingly noticeable compared to the smoke-free baseline. Therefore, an algorithm was developed to automatically detect smoke based on the evolution of the fractal dimension. To perform this analysis reliably, each scenario must include a reference image without smoke and captured under stable weather conditions.

The fractal dimension analysis algorithm consists of two main steps: a computational step and a logical decision step. The first step, detailed in the pseudocode of [Algorithm 1](#), involves calculating the absolute difference in fractal dimension for each corresponding tile between the reference image and the current image. The absolute value is used because the presence of smoke can either increase or decrease the fractal dimension, depending on the characteristics of the original image.

The second step, illustrated in [Fig. 2](#), consists of a logical flow designed to determine whether the new image indicates the presence of fire, based on the output from [Algorithm 1](#). Absolute differences are first compared with a threshold, which is set to the standard deviation of the fractal dimension across all tiles in the reference image σ_{FD} . Tiles with differences greater than the threshold are highlighted using a colour-coded representation (see [Fig. 3](#)) to visually represent (illuminate) the intensity of the deviations. σ_{FD} ranged between 0.04 and 0.06 across the five scenarios of our survey, and the threshold was heuristically set to the minimum value of 0.04, yielding satisfactory results. Determining an optimal threshold based on established academic standards will require broader datasets to obtain statistically significant results, which will be the focus of future analyses.

The flow considers three factors to determine whether a fire is occurring. The first decision block checks whether one or more tiles are illuminated in the incoming image; if none are illuminated, the flow concludes, confirming the absence of fire. The second decision block requires at least five consecutive images with illuminated tiles to indicate a potential fire, reducing the likelihood of false positives caused by external factors. Finally, the third decision block specifies that, for a fire to be identified, no more than three illuminated tiles may appear in the same row and no more than two in the same column. This criterion reflects the typically localised nature of smoke produced by fire and distinguishes it from broader shadows cast by clouds.

4. Results

This section describes the experiments developed in different scenarios. The concept of scenario refers to a collection of images captured from the same position and location under consistent conditions, including pixel dimensions, resolution, dynamic range, bit depth, and other parameters. Additionally, three case studies have been analysed: 1) fire detection under normal conditions; 2) the presence of fog and, 3) cloud shadows. The first case study includes three scenarios focused on fire detection in normal weather conditions. Fog, with its smoke-like texture, can make fire detection more difficult; thus, a specific

scenario to investigate this phenomenon has been considered. Finally, the shadows cast by clouds can alter the image data, potentially affecting the fractal dimension. Therefore, a specific scenario has been designed to investigate this case as well.

[Table 2](#) presents the experimental setup employed in this study. The hardware requirements are relatively low, showing that the method can be implemented on standard computing devices. Additionally, the software employed is both lightweight and open-source, ensuring accessibility and ease of deployment.

[Table 3](#) summarizes the set of general parameters applied across all the scenarios analysed. It first specifies the resolution of the original images in the dataset. Next, it details the matrix dimensions used for the tiling process, including the number of rows and columns and the total number of resulting tiles. Finally, it outlines the parameters used in the fractal dimension calculation algorithm.

Finally, [Table 4](#) presents a number of specific parameters for each scenario. First, the coordinates of the bounding box applied to all images as part of the preprocessing step are given. Additionally, the properties of the original images used in each scenario are detailed, as the dataset is publicly available and the image sizes vary depending on the camera used.

4.1. Results for scenario 1

[Fig. 4](#) illustrates the preprocessing step in Scenario 1. This first scenario consists of six different images ([Fig. 4 \(a-f\)](#)). The first image does not contain smoke; whereas the subsequent images do. The first step identifies the area of interest ([Fig. 4 \(g-l\)](#)). Next, the RGB images are converted to greyscale ([Fig. 4 \(m-r\)](#)). Finally, [Fig. 4 \(s-x\)](#) illustrates the tiling grid, which uses a matrix of 6 rows by 6 columns, yielding a total of 36 tiles.

[Fig. 5](#) shows the evolution of the fractal dimensions before and after the start of the fire. Initially, there are no illuminated tiles in [Fig. 5\(a\)](#). However, as disturbances appear, tiles gradually become illuminated in [Fig. 5 \(b-f\)](#). As previously mentioned, the colour coding represents the intensity of fractal dimension variations. In this case, the algorithm identifies smoke when the conditions are met: a maximum of two illuminated tiles in the same row and two in the same column, some of which persist for more than five consecutive time instants.

4.2. Results for scenario 2

Scenario 2 also consists of six different images ([Fig. 6 \(a-f\)](#)). Here, the fire is further away than in the first scenario, but the amount of smoke is significantly greater. The same preprocessing steps are applied: focusing on the area of interest ([Fig. 6 \(g-l\)](#)), RGB to greyscale conversion ([Fig. 6 \(m-r\)](#)), and tiling ([Fig. 6 \(s-x\)](#)).

In this scenario, the abundant smoke gradually intensifies. [Fig. 7](#) presents the evolution of the fractal dimension-based fire detection. The focal point of the fire appears in [Fig. 7\(b\)](#), but due to the wind, the smoke

Algorithm 1

Pseudo-code for the algorithm to determine smoke using the Fractal Dimension.

Input: OriginalFractalDimensionsList, NewFractalDimensionsList
Output: DifferencesList
Auxiliary Variables: Counter, Difference
Initialization: Counter = 0; Difference = 0; DifferencesList = \emptyset ;

```

1: procedure BEGIN SMOKE DETECTION ALGORITHM
2:   for FractalDimension in NewFractalDimensionsList do
3:     Difference = abs(OriginalFractalDimensionsList[Counter]-FractalDimension)
4:     add(DifferencesList{Counter},Difference)
5:     Counter  $\leftarrow$  Counter + 1
6:   end for
7: end procedure

```

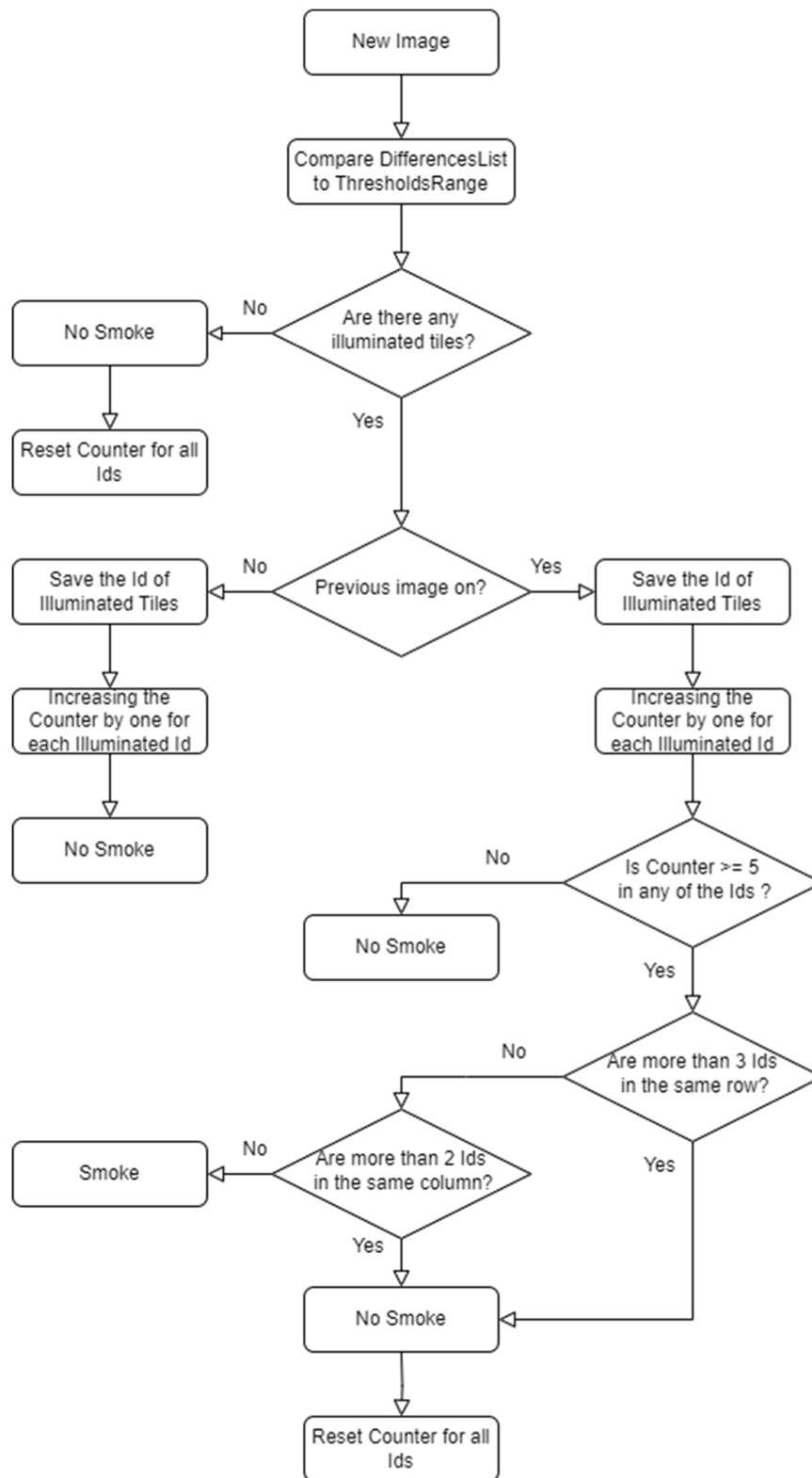


Fig. 2. Flowchart of the fractal dimension evolution analysis algorithm.

expands and illuminates more tiles in Fig. 7 (c–e). In Fig. 7(f), the algorithm detects fire as three tiles are illuminated in the same row and two in the same column. Additionally, the colour coding in red and orange highlights the intensity of the fire.

4.3. Results for scenario 3

The third scenario is the last one that examines the evolution of smoke under normal conditions (Fig. 8 (a–f)). However, this scenario features a distant fire with some haze. Again, preprocessing is performed (see Fig. 8 (g–x)), although the camera position limits the area of interest

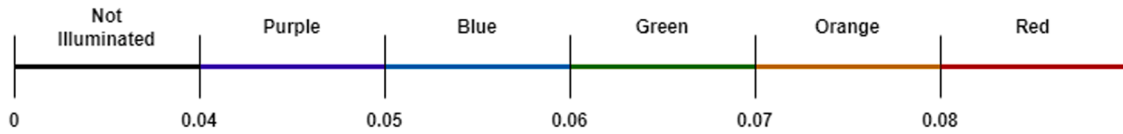


Fig. 3. Colour-coded range of values to illuminate the tiles.

Table 2

Experimental settings.

Experimental Setup	Details
Operating System	Ubuntu 18.04.4 LTS
Image Preprocessing	ImageMagick 6.9.7-4
Fractal Dimension Calculation	Shell Scripting
Smoke Detection Algorithm	Python 3.8.10
CPU	AMD Ryzen 7 5800H
RAM	16,0 GB

Table 3

Generic technical parameters.

Generic Technical Parameters	Details
Original Image Resolution	96 ppp
Number of Rows in Tile Matrix	6
Number of Columns in Tile Matrix	6
Number of Tiles	36
Fractal Dimension Calculation	Compression Fractal Dimension Algorithm
Fractal Dimension Scaling	50 % to 90 %

compared to other scenarios.

Here, the amount and intensity of smoke are significantly less than in the previous case. Haze in the vicinity of the fire further complicates detection. Fig. 9(b) first shows a discrete fire outbreak that moves to the left due to wind (Fig. 9 (c–f)). The algorithm detects smoke as it meets the conditions: a maximum of three illuminated tiles in a row and two in a column. This scenario reflects a low-intensity fire, as indicated by the colour range of the tiles.

4.4. Results for scenario 4

The fourth scenario explores the effect of fog, a weather phenomenon that can complicate smoke detection. Fig. 10 (a–f) shows a series of six images showing the evolution of a distant fire mixed with fog. The preprocessing steps remain the same (Fig. 10(g–x)), but the camera position again limits the area of interest.

As mentioned above, fog is a weather phenomenon that can make fire detection difficult. Fog initially dominates the scene, as shown in Fig. 11(a), with no illuminated tiles. As the fire starts, shown in Fig. 11(b), it blends with the fog but increases the intensity of certain tiles. The wind spreads the fire as shown in Fig. 11 (c–f). The algorithm detects a fire by a maximum of three illuminated tiles in a row, one of which lasts for more than five consecutive time instants. Finally, the colours of the illuminated tiles represent the moderate intensity of this smoke.

Table 4

Specific parameters by scenario.

Parameters by Scenario							
Scenarios		Bounding Box Coordinates				Image Properties	
Number	Type	X Position	Y Position	Box Width	Box Height	Image Size	Total Images
First	Smoke	0	590	20,248	946	2048 × 296	81
Second	Smoke	404	784	2400	1264	2400 × 1264	71
Third	Smoke	302	1132	2512	916	2512 × 916	64
Fourth	Fog Effect	304	1078	2498	970	2498 × 970	64
Fifth	Cloud Shadows	0	719	2048	817	2048 × 817	81

4.5. Results for scenario 5

The fifth scenario shifts the focus from smoke detection to the impact of cloud shadows, a common natural phenomenon that can alter image data and affect fractal dimension analysis. Fig. 12 (a–f) shows the progression of a shadow cast by moving clouds across a landscape. The same preprocessing steps are followed as in the other scenarios (Fig. 12 (g–x)).

Under normal conditions, no tiles are illuminated in Fig. 13(a). However, Fig. 13 (b–c) shows shadows cast by clouds, which significantly alter the fractal dimension and can mimic a false fire. As the clouds continue to move (Fig. 13 (d–f)), some tiles become illuminated before the shadow dissipates. When the number of illuminated tiles exceeds the algorithm's thresholds, the counter resets, indicating no fire. This mechanism prevents false positives, as true fires are typically localised to a group of adjacent tiles and persist for more than five consecutive time instants.

4.6. Comparative validation and discussion

To validate the proposed method across the five scenarios, smoke detection accuracy has been calculated as

$$Accuracy = \frac{TP + TN}{TP + TN + FP + FN} \quad (3)$$

where TP stands for True Positives (number of correctly detected images containing smoke), TN for True Negatives (number of smoke-free images identified as such), FP for False Positives (number of smoke-free images where smoke was detected) and FN , for False Negatives (number of images containing smoke that the method missed). In the end, an accuracy of 96.87 % was achieved in the use cases described, thus fulfilling the purpose of the study. However, it should be noted that in the early stages of a fire, the amount of smoke may not be sufficient to cause significant variations in the fractal dimension. This effect leads to the presence of some false negatives that affect the calculation of the accuracy.

Table 5 shows a comparison of the results with other related works focusing on fire detection in images. Since we do not have access to all the datasets or models, it is not possible to directly assess the accuracy of the method proposed in these works. On the one hand, the table highlights the models used in other studies, with YOLO (You Only Look Once) being the most prominent. In some cases, additional techniques are incorporated to improve performance, such as SAHI (Slicing-Aided Hyper Inference). On the other hand, it is clear that Artificial Intelligence (AI)-based fire detection models require a large number of images for effective training. Finally, when AI-based object detectors are involved, related metrics are employed to measure accuracy, including

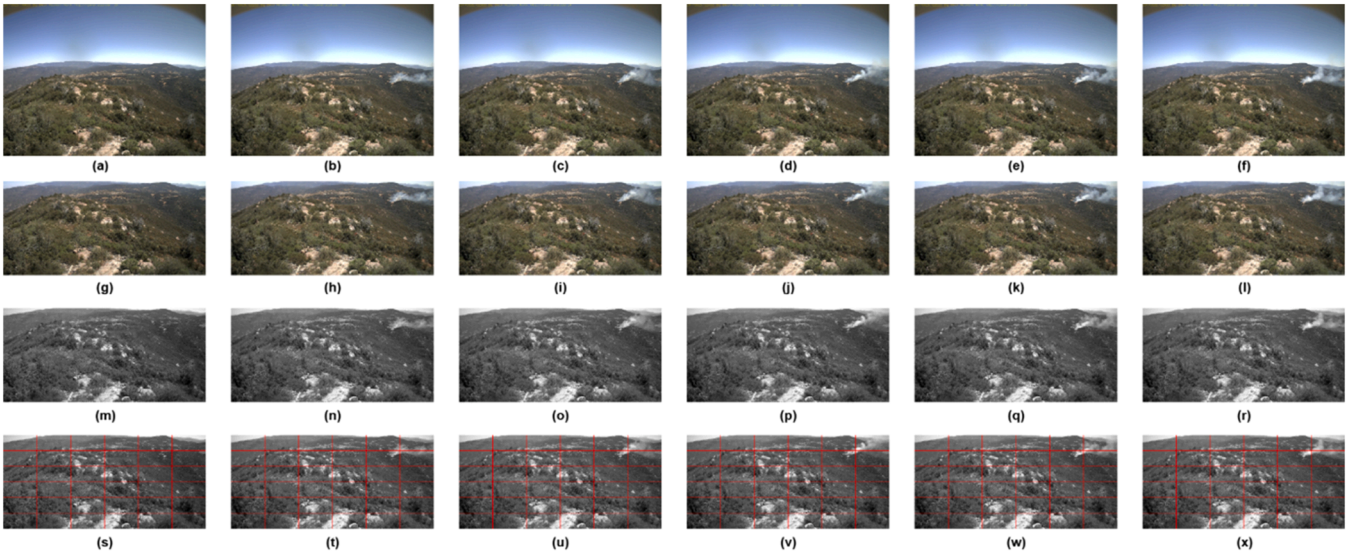


Fig. 4. First scenario preprocessing.

(a) Initial RGB Image (image 1). (b) Initial RGB Image (image 2). (c) Initial RGB Image (image 3). (d) Initial RGB Image (image 4). (e) Initial RGB Image (image 5). (f) Initial RGB Image (image 6). (g) Initial RGB Image cropped (image 1). (h) Initial RGB Image cropped (image 2). (i) Initial RGB Image cropped (image 3). (j) Initial RGB Image cropped (image 4). (k) Initial RGB Image cropped (image 5). (l) Initial RGB Image cropped (image 6). (m) Cropped Greyscale (image 1). (n) Cropped Greyscale (image 2). (o) Cropped Greyscale (image 3). (p) Cropped Greyscale (image 4). (q) Cropped Greyscale (image 5). (r) Cropped Greyscale (image 6). (s) Cropped Greyscale Tiled (image 1). (t) Cropped Greyscale Tiled (image 2). (u) Cropped Greyscale Tiled (image 3). (v) Cropped Greyscale Tiled (image 4). (w) Cropped Greyscale Tiled (image 5). (x) Cropped Greyscale Tiled (image 6).

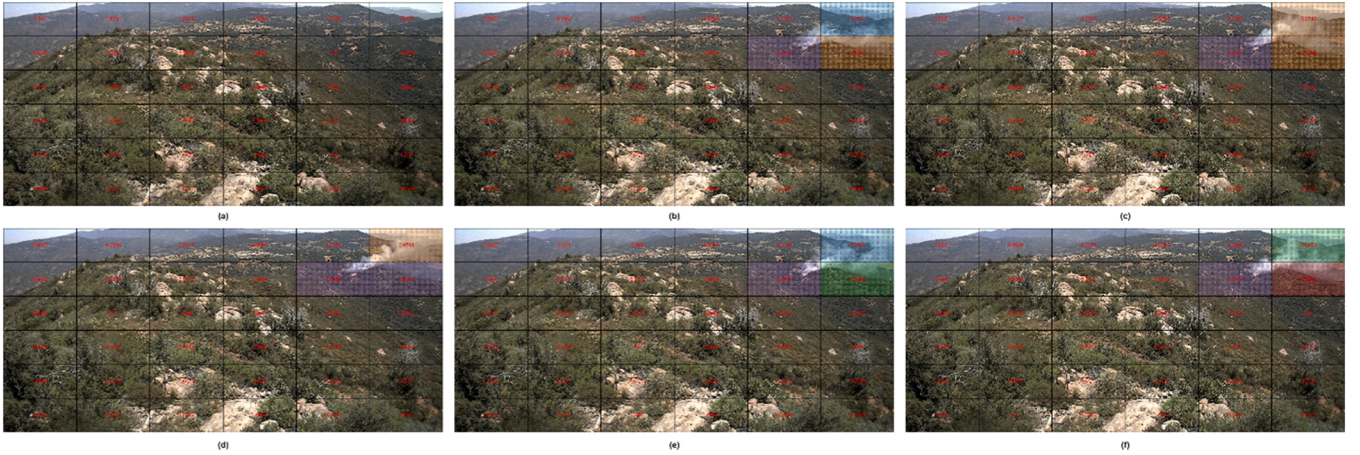


Fig. 5. Evolution of fractal dimension in Scenario 1.

(a) Initial RGB Image Cropped (image 1). (b) Initial RGB Image Cropped (image 2). (c) Initial RGB Image Cropped (image 3). (d) Initial RGB Image Cropped (image 4). (e) Initial RGB Image Cropped (image 5). (f) Initial RGB Image Cropped (image 6).

AP (Average Precision) and IoU (Intersection over Union), alongside the approach used in this work.

After analyzing the results of this study, several limitations can be identified. Firstly, the study is based on a public dataset with images of limited quality, which introduces noise into the calculation of the fractal dimension. In addition, this study has two essential requirements. First, a reference image of the monitored scene under normal conditions needs to be available and updated when the environment changes. Secondly, a static image acquisition system is required, without zooming in or out. Finally, as previously mentioned, during the early stages of a fire, the amount of smoke may be insufficient to cause significant variations in the fractal dimension, potentially delaying the activation of the algorithm.

5. Conclusion

This paper presents a smoke detection method based on fractal dimension calculation using images from the High Performance Wireless Research and Education Network surveillance network, which consists of cameras positioned on hillsides. The proposed approach is straightforward and involves dividing the images into tiles, calculating the fractal dimension for each tile, and then analysing the distribution of these values. As the images contain elements that could introduce outliers, such as the sky and camera edges, a predefined cropping step is applied to ensure consistency. The cropped images are then converted to greyscale, as this increases the accuracy of the fractal dimension calculation by exploiting the wide range of intermediate grey values available in each pixel. The size of the tiling matrix is a crucial parameter that is adjusted according to the resolution and dimensions of the processed image. The method, which is based on the computational

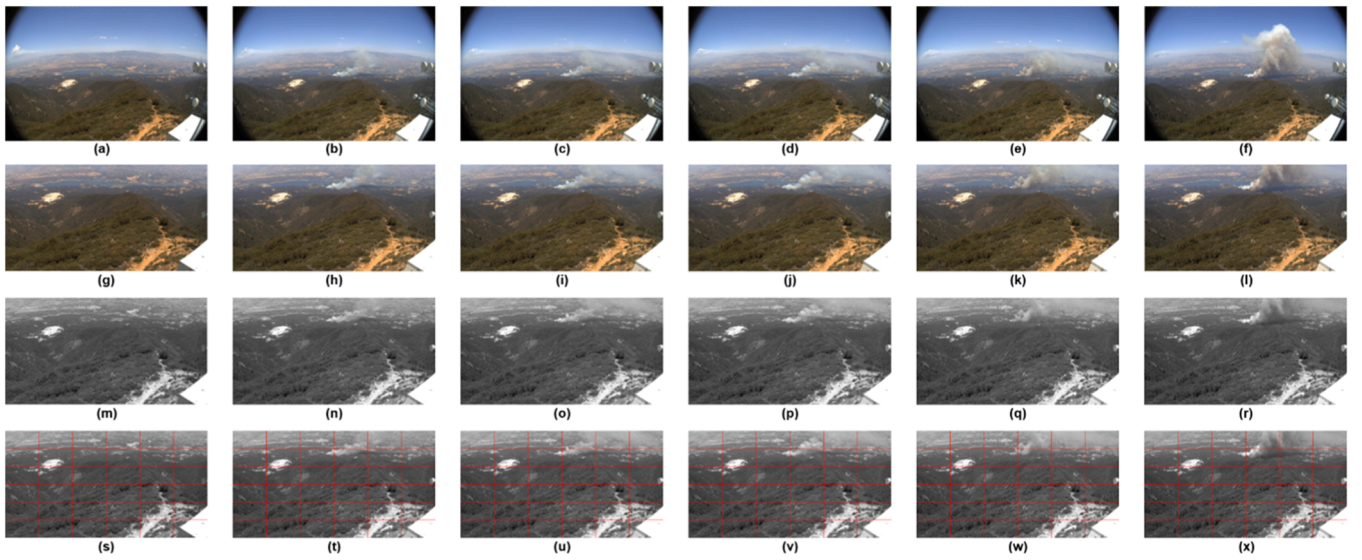


Fig. 6. Second scenario preprocessing.

(a) Initial RGB Image (image 1). (b) Initial RGB Image (image 2). (c) Initial RGB Image (image 3). (d) Initial RGB Image (image 4). (e) Initial RGB Image (image 5). (f) Initial RGB Image (image 6). (g) Initial RGB Image cropped (image 1). (h) Initial RGB Image cropped (image 2). (i) Initial RGB Image cropped (image 3). (j) Initial RGB Image cropped (image 4). (k) Initial RGB Image cropped (image 5). (l) Initial RGB Image cropped (image 6). (m) Cropped Greyscale (image 1). (n) Cropped Greyscale (image 2). (o) Cropped Greyscale (image 3). (p) Cropped Greyscale (image 4). (q) Cropped Greyscale (image 5). (r) Cropped Greyscale (image 6). (s) Cropped Greyscale Tiled (image 1). (t) Cropped Greyscale Tiled (image 2). (u) Cropped Greyscale Tiled (image 3). (v) Cropped Greyscale Tiled (image 4). (w) Cropped Greyscale Tiled (image 5). (x) Cropped Greyscale Tiled (image 6).

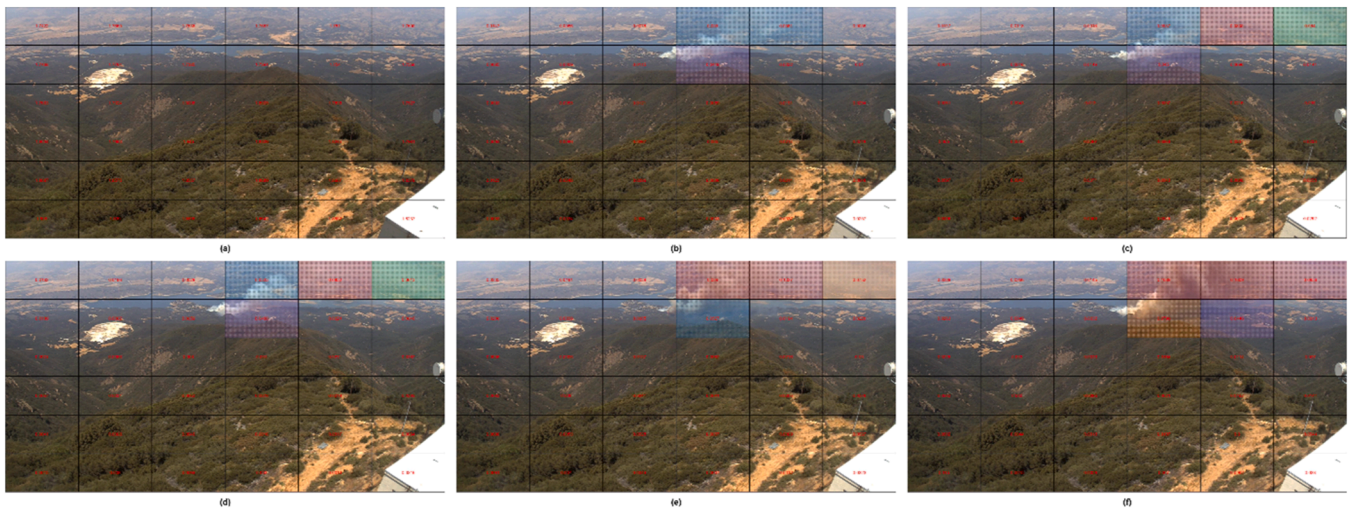


Fig. 7. Evolution of fractal dimension in Scenario 2.

(a) Initial RGB Image Cropped (image 1). (b) Initial RGB Image Cropped (image 2). (c) Initial RGB Image Cropped (image 3). (d) Initial RGB Image Cropped (image 4). (e) Initial RGB Image Cropped (image 5). (f) Initial RGB Image Cropped (image 6).

scheme described in [1] for estimating fractal dimensions from digital image files, is highly efficient. Once the fractal dimension of each tile has been calculated, an evolutionary analysis is performed to detect smoke within images of the same scenario. Since smoke reduces texture contrast and changes the fractal dimension, its presence causes noticeable differences in certain tiles compared to smoke-free conditions. Based on this observation, an algorithm has been developed to automatically detect smoke by tracking the evolution of the fractal dimension values, with an accuracy of 96.87 %. The main contribution of this research is that, unlike other related work, it presents an efficient and accurate method capable of using the texture of smoke in images to detect forest fires, regardless of weather conditions such as cloud shadows or fog.

In light of the above, the main theoretical and practical implications

of the present work are as follows:

Fractal dimension and image analysis: This research highlights the potential of fractal dimension as a powerful tool for texture analysis in images. By extending the theoretical framework of fractals to the image compression domain, our study demonstrates that the presence of smoke alters image texture in a measurable way—captured effectively through fractal dimension metrics. This finding is significant, as it illustrates how a concept traditionally used to describe self-similarity and complexity in mathematical and physical systems can be successfully applied to real-world image data, particularly in the context of environmental monitoring.

Understanding texture variations caused by smoke presence: This study offers new insights into how smoke affects image texture, positioning texture as a valuable feature for developing fire detection

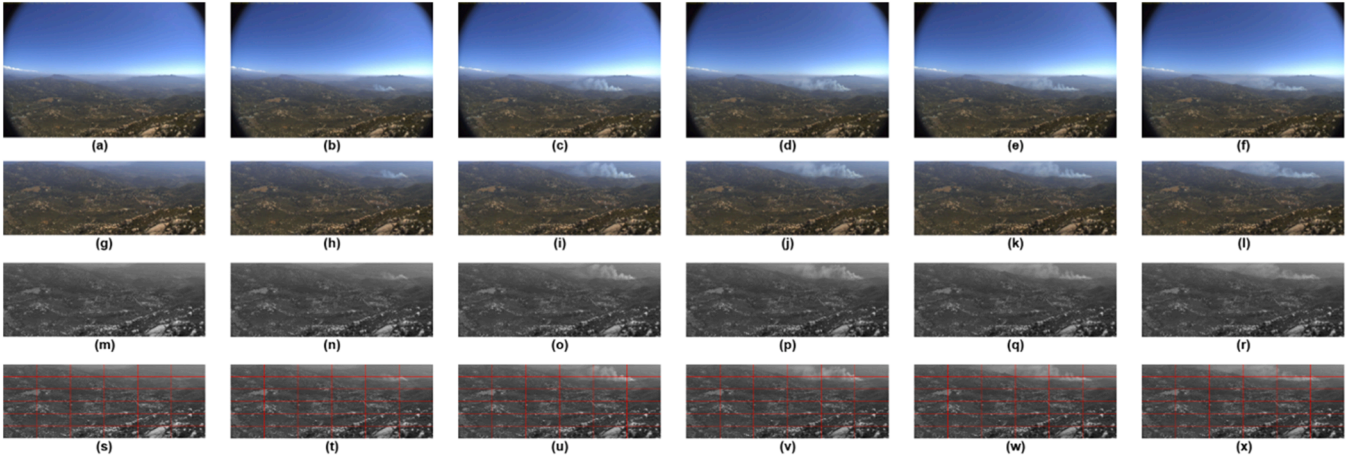


Fig. 8. Third scenario preprocessing.

(a) Initial RGB Image (image 1). (b) Initial RGB Image (image 2). (c) Initial RGB Image (image 3). (d) Initial RGB Image (image 4). (e) Initial RGB Image (image 5). (f) Initial RGB Image (image 6). (g) Initial RGB Image cropped (image 1). (h) Initial RGB Image cropped (image 2). (i) Initial RGB Image cropped (image 3). (j) Initial RGB Image cropped (image 4). (k) Initial RGB Image cropped (image 5). (l) Initial RGB Image cropped (image 6). (m) Cropped Greyscale (image 1). (n) Cropped Greyscale (image 2). (o) Cropped Greyscale (image 3). (p) Cropped Greyscale (image 4). (q) Cropped Greyscale (image 5). (r) Cropped Greyscale (image 6). (s) Cropped Greyscale Tiled (image 1). (t) Cropped Greyscale Tiled (image 2). (u) Cropped Greyscale Tiled (image 3). (v) Cropped Greyscale Tiled (image 4). (w) Cropped Greyscale Tiled (image 5). (x) Cropped Greyscale Tiled (image 6).

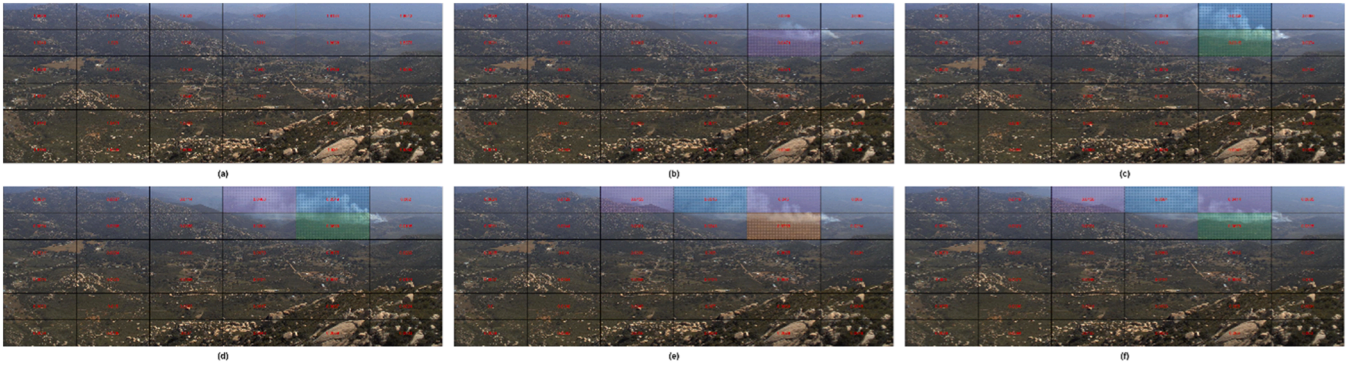


Fig. 9. Evolution of fractal dimension in Scenario 3.

(a) Initial RGB Image Cropped (image 1). (b) Initial RGB Image Cropped (image 2). (c) Initial RGB Image Cropped (image 3). (d) Initial RGB Image Cropped (image 4). (e) Initial RGB Image Cropped (image 5). (f) Initial RGB Image Cropped (image 6).

algorithms. It establishes a theoretical link between smoke and fractal dimension, demonstrating that the presence of smoke reduces texture contrast, which in turn leads to measurable changes in the fractal dimension of the affected image regions.

Evolution analysis of fractal dimension: This allows for tracking of smoke evolution over time and could be easily extended to various other applications in environmental monitoring, where changes over time are crucial.

Efficient smoke detection: This research presents a practical and computationally efficient method for detecting smoke in images using fractal dimension analysis. By focusing on texture changes in greyscale images, the approach offers a simple yet effective means of identifying smoke, making it well-suited for integration into fire monitoring systems with minimal computational load.

Real-world applicability: The ability of the proposed method to function under different environmental conditions (such as cloud shadows or fog) enhances its practical applicability. This is a significant advantage as many existing fire detection systems are often hindered by weather-related challenges [4,6–9,11]. The weather robustness of the algorithm could make it more reliable in different environments, which is essential for global deployment in forest fire management and disaster response.

Evolution analysis for continuous monitoring: By focusing on the evolution of fractal dimension values, the method can continuously monitor and update smoke detection status over time, making it ideal for automated monitoring networks such as HPWREN. This means that fire detection could be achieved in near real time, allowing faster responses to emerging fire threats.

In conclusion, this research bridges theoretical concepts (fractal dimension) and practical applications (fire detection) in environmental monitoring. It proposes an efficient and scalable method for smoke detection in images, with great potential for improving real-time fire detection systems.

When analysing the advantages of this work, complexity is a main factor to be considered, especially when compared to methods based in Artificial Intelligence, which involve much more resource-intensive tasks. In addition, the method presented in this paper requires only the source image, without any specific data source requirements, such as geoinformation metadata, which is highly advantageous. Finally, the experimental results obtained from images of five different scenarios show that the proposed method effectively discriminates areas with smoke and smoke-free, not only under normal conditions but also in the presence of fog and cloud shadows.

It is important to acknowledge the limitations of the proposed

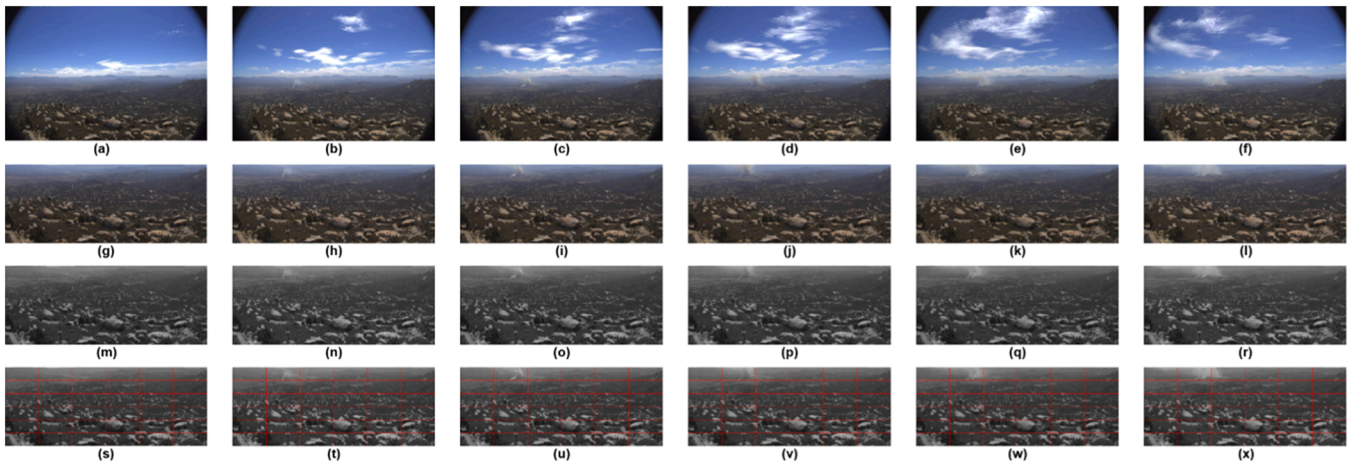


Fig. 10. Fourth scenario preprocessing.

(a) Initial RGB Image (image 1). (b) Initial RGB Image (image 2). (c) Initial RGB Image (image 3). (d) Initial RGB Image (image 4). (e) Initial RGB Image (image 5). (f) Initial RGB Image (image 6). (g) Initial RGB Image cropped (image 1). (h) Initial RGB Image cropped (image 2). (i) Initial RGB Image cropped (image 3). (j) Initial RGB Image cropped (image 4). (k) Initial RGB Image cropped (image 5). (l) Initial RGB Image cropped (image 6). (m) Cropped Greyscale (image 1). (n) Cropped Greyscale (image 2). (o) Cropped Greyscale (image 3). (p) Cropped Greyscale (image 4). (q) Cropped Greyscale (image 5). (r) Cropped Greyscale (image 6). (s) Cropped Greyscale Tiled (image 1). (t) Cropped Greyscale Tiled (image 2). (u) Cropped Greyscale Tiled (image 3). (v) Cropped Greyscale Tiled (image 4). (w) Cropped Greyscale Tiled (image 5). (x) Cropped Greyscale Tiled (image 6).

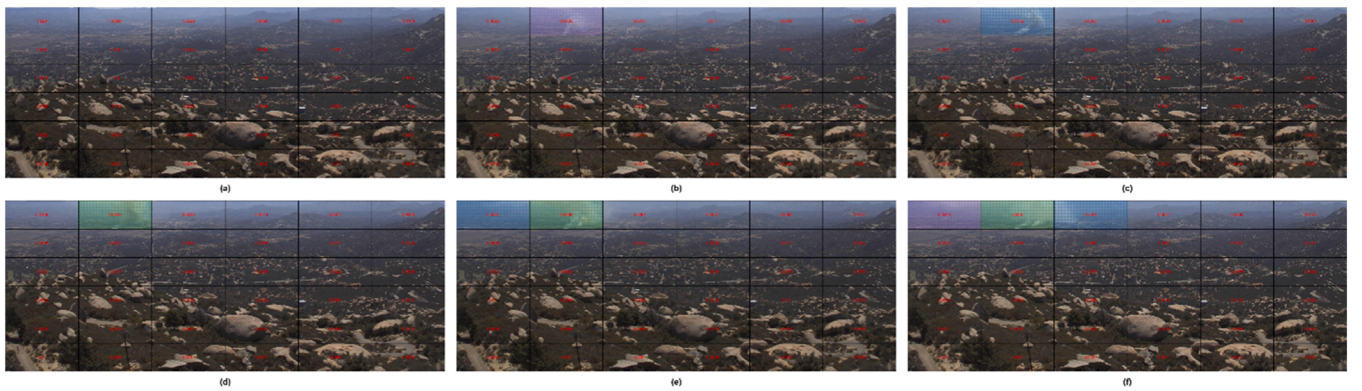


Fig. 11. Evolution of fractal dimension in Scenario 4.

(a) Initial RGB Image Cropped (image 1). (b) Initial RGB Image Cropped (image 2). (c) Initial RGB Image Cropped (image 3). (d) Initial RGB Image Cropped (image 4). (e) Initial RGB Image Cropped (image 5). (f) Initial RGB Image Cropped (image 6).

method. In the early stages of a fire, the amount of smoke present may be insufficient to induce significant changes in fractal dimension, potentially reducing the sensitivity of the detection method. Moreover, the current approach relies on static images and assumes the availability of an updated reference image captured under normal conditions for each scenario.

As a future research direction, we aim at exploring the capability of the system to operate with dynamic, non-static images, by including an initial pre-processing step involving registration of acquired images. In addition, we aim to test the method on different platforms (e.g., drones, satellites, fixed surveillance) to assess its generalisability and performance under different resolutions and perspectives. Along this line, another possibility is to explore the implementation of the method on edge computing devices for decentralised and low-latency smoke detection, which could open up practical applications in wildfire monitoring systems. Future research could also investigate the use of adaptive tile sizes based on image content to improve sensitivity in regions where smoke features are more prominent or subtle. Another possibility is to explore the combination of the fractal dimension with additional texture or edge-based features to improve robustness in complex environments and to further distinguish smoke from similar-

looking artefacts such as fog or dust. Finally, another possibility is to investigate the potential of combining fractal dimension features with lightweight Machine Learning classifiers (e.g., Support Vector Machines, decision trees) to improve smoke detection while keeping computational costs low compared to Deep Learning approaches.

Funding

The work was partly supported by the Department of Education, Junta de Castilla y León, grant VA184P24 and FEDER Funds (Reference: CLU-2023-1-05) and by the EU Horizon 2020 Research and Innovation Programme under the Marie Skłodowska-Curie grant agreement No 101,008,297. This article reflects only the authors' view. The European Union Commission is not responsible for any use that may be made of the information it contains.

Data availability

All the experiments in this paper have been carried out using data available at [2]. Access conditions are defined therein.

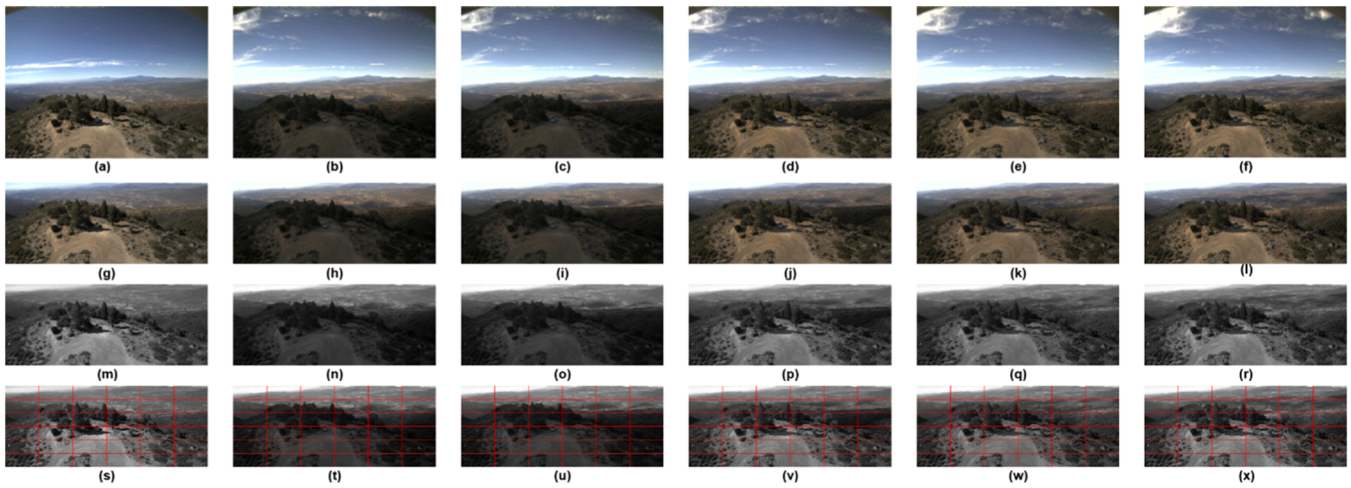


Fig. 12. Fifth scenario preprocessing.

(a) Initial RGB Image (image 1). (b) Initial RGB Image (image 2). (c) Initial RGB Image (image 3). (d) Initial RGB Image (image 4). (e) Initial RGB Image (image 5). (f) Initial RGB Image (image 6). (g) Initial RGB Image cropped (image 1). (h) Initial RGB Image cropped (image 2). (i) Initial RGB Image cropped (image 3). (j) Initial RGB Image cropped (image 4). (k) Initial RGB Image cropped (image 5). (l) Initial RGB Image cropped (image 6). (m) Cropped Greyscale (image 1). (n) Cropped Greyscale (image 2). (o) Cropped Greyscale (image 3). (p) Cropped Greyscale (image 4). (q) Cropped Greyscale (image 5). (r) Cropped Greyscale (image 6). (s) Cropped Greyscale Tiled (image 1). (t) Cropped Greyscale Tiled (image 2). (u) Cropped Greyscale Tiled (image 3). (v) Cropped Greyscale Tiled (image 4). (w) Cropped Greyscale Tiled (image 5). (x) Cropped Greyscale Tiled (image 6).

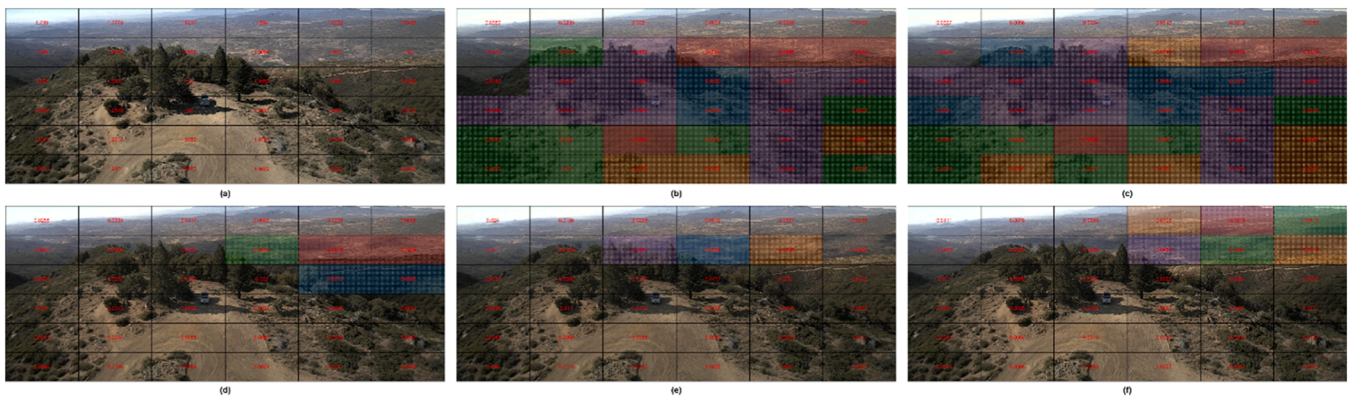


Fig. 13. Evolution of fractal dimension in Scenario 5. (a) Initial RGB Image Cropped (image 1). (b) Initial RGB Image Cropped (image 2). (c) Initial RGB Image Cropped (image 3). (d) Initial RGB Image Cropped (image 4). (e) Initial RGB Image Cropped (image 5). (f) Initial RGB Image Cropped (image 6).

Table 5

Comparison results.

Reference	Model	Dataset Length	Accuracy
[4]	YOLOv5s	2554 images	96 % AP50 and 57.3 % AP50:95
[5]	MobileNetV3	2700 images	87.66 %
[6]	U-Net Base	22,500 images	95.31 % IoU
[7]	YOLOv8	10,000 images	79.30 %
[9]	YOLOv8 + SAHI	11,515 images	92.20 %
[10]	YOLOv5	30,420 images	92.10 % AP50
[8]	YOLOv8	11,000 images	87.10 % AP50 and 82.40 % AP75
[11]	Deeplabv3+	9098 images	90.41 %
Present Study	Fractal Dimension	316 images	96.87 %

CRediT authorship contribution statement

Javier Del-Pozo-Velázquez: Formal analysis, Software, Visualization, Writing – original draft, Writing – review & editing. **Javier Manuel Aguiar-Pérez:** Conceptualization, Methodology, Funding acquisition, Supervision. **Pedro Chamorro-Posada:** Conceptualization, Methodology, Funding acquisition, Supervision. **María Ángeles Pérez-Juárez:** Validation, Writing – original draft, Writing – review & editing. **Xin-heng Wang:** Methodology. **Pablo Casaseca-de-la-Higuera:** Methodology, Writing – review & editing, Funding acquisition.

Declaration of competing interest

The authors declare that they have no known competing financial interests or personal relationships that could have appeared to influence the work reported in this paper.

References

- [1] P. Chamorro-Posada, A simple method for estimating the fractal dimension from digital images: the compression dimension, *Chaos. Solitons. Fractals*. 91 (2016) 562–572, <https://doi.org/10.1016/j.chaos.2016.08.002>.

- [2] HPWREN, 2025. <https://www.hpwren.ucsd.edu/> [accessed 10 April 2025].
- [3] J. Wu, *Introduction to Convolutional Neural Networks*, National Key Lab for Novel Software Technology, China, 2017.
- [4] H. Yang, J. Wang, J. Wang, Efficient detection of forest fire smoke in UAV aerial imagery based on an improved YOLOv5 model and Transfer Learning, *Remote Sens. (Basel)* 15 (23) (2023) 5527, <https://doi.org/10.3390/rs15235527>.
- [5] I. El-Madafri, M. Peña, N. Olmedo-Torre, The wildfire dataset: enhancing deep learning-based forest fire detection with a diverse evolving open-source dataset focused on data representativeness and a novel multi-task learning approach, *Forests* 14 (9) (2023) 1697, <https://doi.org/10.3390/f14091697>.
- [6] T.F. Ribeiro, F. Silva, J. Moreira, R.L. De C. Costa, Burned area semantic segmentation: a novel dataset and evaluation using convolutional networks, *ISPRS J. Photogramm. Remote Sens.* 202 (2023) 565–580, <https://doi.org/10.1016/j.isprsjprs.2023.07.002>.
- [7] Lostanlen M., Veith F., Buc C., Barriere V. Scrapping the web for early wildfire detection. *arXiv (Cornell University)* 2024. <https://doi.org/10.48550/arxiv.2402.05349>.
- [8] S. Ma, W. Li, L. Wan, G. Zhang, A lightweight fire detection algorithm based on the improved YOLOv8 Model, *Appl. Sci.* 14 (16) (2024) 6878, <https://doi.org/10.3390/app14166878>.
- [9] M. Ishtiaq, J. Won, YOLO-SIFD: YOLO with sliced inference and fractal dimension analysis for improved fire and smoke detection, *Comput. Mater. Continua.* 82 (3) (2025) 5343–5361, <https://doi.org/10.32604/cmc.2025.061466>.
- [10] J. Qian, J. Lin, D. Bai, R. Xu, H. Lin, Omni-dimensional dynamic convolution meets bottleneck transformer: a novel improved high accuracy forest fire smoke detection model, *Forests* 14 (4) (2023) 838, <https://doi.org/10.3390/f14040838>.
- [11] A. Kumar, A. Perrusquía, S. Al-Rubaye, W. Guo, Wildfire and smoke early detection for drone applications: a light-weight Deep learning approach, *Eng. Appl. Artif. Intell.* 136 (2024) 108977, <https://doi.org/10.1016/j.engappai.2024.108977>.
- [12] J. Kang, S. Tariq, H. Oh, S.S. Woo, A survey of Deep Learning-based object detection methods and datasets for overhead imagery, *IEEe Access.* 10 (2022) 20118–20134.
- [13] J. Ghahremani Nahr, H. Nozari, M.E. Sadeghi, Artificial intelligence and machine learning for real-world problems (a survey), *Int. J. Innov. Eng.* 1 (3) (2021) 38–47.
- [14] A. Garg, A. Agrawal, A. Negi, A review on natural phenomenon of fractal geometry, *Int. J. Comput. Appl.* 86 (4) (2014) 975–8887, <https://doi.org/10.5120/14970-3157>.
- [15] M. Nurujjaman, A. Hossain, P. Ahmed, A review of fractals properties: mathematical approach, *Sci. J. Appl. Math. Stat.* 5 (3) (2017) 98–105, <https://doi.org/10.11648/j.sjams.20170503.11>.
- [16] D. Kolyukhin, Study the accuracy of the correlation fractal dimension estimation, *Commun. Stat - Simul. Comput.* (2021), <https://doi.org/10.1080/03610918.2021.2014888>.
- [17] W. Zhao, J. Yan, G. Hou, P. Diwu, T. Liu, J. Hou, R. Li, Research on a fractal dimension calculation method for a nano-polymer microspheres dispersed system, *Front. Chem.* 9 (2021) 732797, <https://doi.org/10.3389/fchem.2021.732797>.
- [18] F.M. Mwema, T.C. Jen, P. Kaspar, Fractal theory in thin films: literature review and bibliometric evidence on applications and trends, *Fractal. Fract.* 6 (2022) 489, <https://doi.org/10.3390/fractalfract6090489>.
- [19] T. Marquardt, A.W. Momber, The determination of fractal dimensions of blast-cleaned steel substrates by means of comparative cross-section image analysis and contact stylus instrument measurements, *J. Adhes. Sci. Technol.* (2022), <https://doi.org/10.1080/01694243.2022.2118567>.
- [20] T. Naito, Y. Fukuda, The universal relationship between sample dimensions and cooperative phenomena: effects of fractal dimension on the electronic properties of high-Tc cuprate observed using electron spin resonance, *Phys. Chem. Chem. Phys.* 24 (2022) 4147–4156.
- [21] J. Sánchez, M. Martín-Landrove, Morphological and fractal properties of brain tumors, *Front. Physiol.* (2022), <https://doi.org/10.3389/fphys.2022.878391>.
- [22] X. Hu, H. Liu, X. Tan, C. Yi, Z. Niu, J. Li, J. Li, Image recognition-based identification of multifractal features of faults, *Front. Earth. Sci.* (2022), <https://doi.org/10.3389/feart.2022.909166>.
- [23] C. Porcaro, M. Marino, S. Carozzo, M. Russo, M. Ursino, V. Ruggiero, C. Ragno, S. Proto, P. Tonin, Fractal dimension feature as a signature of severity in disorders of consciousness: an EEG study, *Int. J. Neural Syst.* 32 (7) (2022) 2250030, <https://doi.org/10.1142/S0129065722500319>.
- [24] P. Kaler, Study of greyscale image in image processing, *Int. J. Recent Innov. Trends Comput. Commun.* 4 (11) (2016) 309–311, <https://doi.org/10.17762/ijritcc.v4i11.2653>.
- [25] S.R. Nayak, J. Mishra, An improved method to estimate the fractal dimension of color images, *Perspect. Sci.* 8 (2016) 412–416, <https://doi.org/10.1016/j.pisc.2016.04.092>, issn: 2213-0209.
- [26] G. Perrolas, M. Niknejad, R. Ribeiro, A. Bernardino, Scalable fire and smoke segmentation from aerial images using convolutional neural networks and quad-tree search, *Sensors* 22 (2022) 1701, <https://doi.org/10.3390/s22051701>.
- [27] ImageMagick, 2025. <https://imagemagick.org/index.php> [accessed 10 April 2025].